NOISE TEMPERATURE AND SENSITIVITY OF A NbN HOT-ELECTRON MIXER AT FREQUENCIES FROM 0.7 THz TO 5.2 THz

J. Schubert[1], A. Semenov[2], G. Gol'tsman[2], H.-W. Hübers[1], G. Schwaab[3], B. Voronov[2], E. Gershenzon[2],

[1] DLR Institute of Space Sensor Technology, Rudower Chaussee 5, 12489 Berlin, Germany
[2] Physical Department, State Pedagogical University, 119435 Moscow, Russia
[3] Physical Chemistry Department II, Ruhr University Bochum, 44801 Bochum, Germany

Abstract

We report on noise temperature measurements of a NbN phonon-cooled hot-electron bolometric mixer at different bias regimes. The device was a 3 nm thick bridge with in-plane dimensions of 1.7 x 0.2 μm^2 integrated in a complementary logarithmic spiral antenna. Measurements were performed at frequencies ranging from 0.7 THz up to 5.2 THz. The measured DSB noise temperatures are 1500 K (0.7 THz), 2200 K (1.4 THz), 2600 K (1.6 THz), 2900 K (2.5 THz), 4000 K (3.1 THz) 5600 K (4.3 THz) and 8800 K (5.2 THz). Two bias regimes are possible in order to achieve low noise temperatures. But only one of them yields sensitivity fluctuations close to the theoretical limit.

1. Introduction

High resolution heterodyne spectroscopy in the frequency range from 1 to 6 THz yields important information on astronomical objects as well as on the chemical composition of the atmosphere of the earth. Some prominent examples are the CII fine structure line at 1.6 THz and the OI fine structure line at 4.75 THz which are major coolant lines of the interstellar medium. The OH rotational transitions at 2.5 THz and 3.5 THz allow for the determination of the OH volume mixing ratio in the stratosphere and gives important information on the catalytic cycles which are responsible for the destruction of stratospheric ozone. A number of on-going astrophysical and atmospheric research programs are aimed at these goals.

So far Schottky diodes have commonly been used as mixers in heterodyne receivers at frequencies above 1.2 THz. The achieved double sideband (DSB) receiver noise temperatures range from 2500 K at 1 THz to about 70000 K at 4.75 THz [1,2]. These numbers are far above the quantum noise limit. However, many research and observation goals require a receiver noise temperature close to the quantum limit. Superconducting hot-electron bolometric (HEB) mixers are prominent devices in order to satisfy this requirement. In the following we report on the results of noise temperature measurements performed with the same phonon-cooled NbN HEB mixer at seven frequencies from 0.7 THz to 5.2 THz.

2. Mixer Design

The investigated HEB was made from a 3 nm thick superconducting NbN film. The film was deposited by dc reactive magnetron sputtering onto a 350 μm thick high resistivity Si substrate (5 kΩ cm). The details of the process are described elsewhere [3]. The bolometer itself is a 1.7 μm wide and 0.2 μm long bridge; it has a transition temperature of 9.3 K and a 870 μΩ cm resistivity at room temperature.

A planar two-arm logarithmic-spiral antenna is used to couple both the signal and the local oscillator (LO) radiation with the bolometer (fig. 1). The central part of the antenna was patterned using electron beam lithography while the outer part was defined by conventional UV photolithography (for details see Ref. [4]). The circle, inside which the antenna arms formed inner terminals and seized to represent a spiral, has 2.6 μm diameter. The diameter of the circle that circumscribes the spiral structure is 130 μm. Between these circles, the antenna arms make two full turns. A radial line from the origin of the antenna intersects a spiral arm at an angle of 70°. The spiral structure terminates a coplanar line that has an impedance of 50 Ω and was lithographed on the same substrate. According to estimates [5], such an antenna should have rf impedance of about 75 Ω when suspended in free space. We expect an even smaller value for our antenna since it is supported by the semi-infinite dielectric half-space simulated by the substrate with the thickness much larger than the wavelength.

The substrate supporting the HEB with the planar antenna was glued onto the flat side of an extended hyperhemispheric lens. The lens was cut off from an optically polished 6 mm diameter sphere that was made from high resistivity (>10 kΩ cm) silicon. No antireflection coating was used. The extension of the lens together with the substrate yields a total extension length of 1.2 mm. This is very close to the optimal extension length for which the beam pattern of the hybrid antenna is diffraction limited, i.e. the pattern is rather determined by the diameter of the lens than by the beam properties of the planar feed antenna. In this case the side-lobes are still low. It is worth mentioning that in the range of the diameter to wavelength ratios,

which we covered in the experiment, the optimal extension length is almost independent on the wavelength [6].

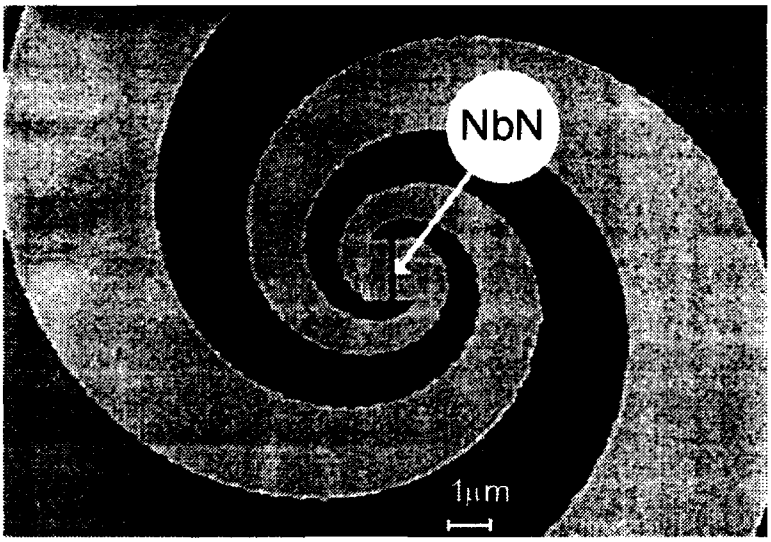

Fig. 1: SEM picture of the inner part of the spiral antenna with the NbN HEB.

3. Experimental Setup

The lens and the HEB were mounted in a copper holder which in turn was directly screwed to the 4.2 K cold plate of an Infrared Labs HD-3 LHe cryostat. The cryostat has a wedged 1.5 mm thick TPX pressure window. A 1.2 mm thick quartz window with an antireflection coating was mounted on the 77 K shield. This filter has a cut-off frequency exceeding 6 THz. The intermediate frequency (IF) signal was guided out of the HEB via a 50 Ω coplanar line, which was soldered to SMA connector. A bias tee followed by an isolator was used to feed the bias to the mixer and to transmit the IF signal to a low noise (< 3 K) 1.2 - 1.8 GHz HEMT amplifier (36 dB gain at 1.5 GHz). Bias tee, isolator and amplifier were also mounted on the cold plate of the cryostat. The output of the amplifier was filtered at 1.5 GHz with a bandwidth of 75 MHz, further amplified and finally detected with a crystal detector.

The device was investigated at seven different frequencies ranging from 0.7 THz up to 5.2 THz. Two FIR gas laser systems were used to cover this frequency region. The measurements from 0.7 THz to 2.5 THz were performed using an optically pumped FIR ring laser [7]. The ring laser design prevents back-reflection of CO_2 pump radiation from the FIR cavity into the CO_2 laser cavity resulting in a stable output power of the FIR laser. Out-coupling of FIR radiation was performed through a 3 mm

diameter hole in one of the laser mirrors. For the measurements between 2.5 THz and 5.2 THz a transversely excited FIR laser was used. As it is the case for the ring laser this design inhibits the back-reflection of CO_2 radiation into the pump laser. For this laser a 45° moveable mirror was used for the output coupling of the FIR radiation. This mirror can be moved transversely to the optical axis of the FIR laser and allows for optimization of the output power for each laser line separately [8]. It should be mentioned that the noise temperature measured at 2.52 THz was the same independently on which laser system was used for the measurements.

Freq. [THz]	0.6929	1.3971	1.6266	2.5228	3.1059	4.2517	5.2456
Lasing medium	HCOOH	CH_2F_2	CH_2F_2	CH_3OH	CH_3OH	CH_3OH	CH_3OD
CO_2 pump line	9R20	9R34	9R32	9P36	9R10	9P34	9R8

Table 1: The laser lines used for the investigations.

The output radiation of the ring laser (see fig. 2) was focussed onto the HEB mixer by two high-density polyethylene lenses (one lens for the setup with the transversely excited FIR laser). In order to monitor the LO output power a wire grid in the LO beam path deflected a minor fraction of the LO radiation onto a pyroelectric detector. A second, rotatable wire grid served for attenuation of the LO power delivered to the HEB. The signal and the LO beam were superimposed by a 6 μm thick Mylar beamsplitter.

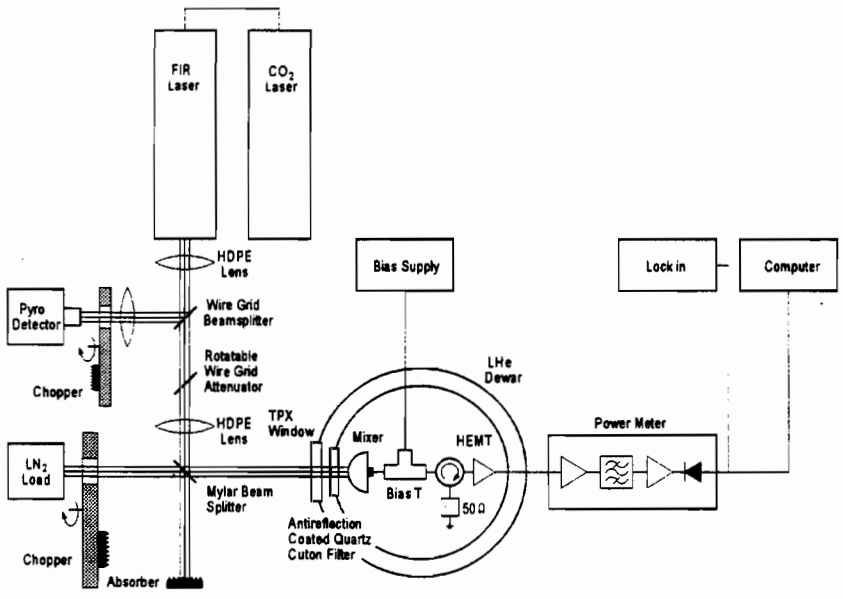

Fig. 2: Experimental setup.

Double sideband (DSB) receiver noise temperatures were determined by the Y-factor method. Ecosorb was used as the hot and cold load. The temperature of the hot and cold load was 293 K and 77 K, respectively. The stability of the laser systems was good enough to measure the noise temperature by putting alternately the hot load and the cold load for about ten seconds in the signal path behind the beamsplitter. The not evacuated optical path from the load to the pressure window of the cryostat was about 25 cm long. The hot and cold reading were averaged by a computer and the Y-factor as well as the noise temeperature were calculated. Due to the relatively weak laser line and the narrow line profile the noise temperature at 5.2 THz was measured by chopping (frequency: 15 Hz) between the hot and cold load using lock-in technique. It was verified at the other frequencies that the direct technique and the chopping technique yield the same result At frequencies above 1 THz the Rayleigh-Jeans approximation does no longer closely describe the power radiated by a black body into a single mode. Therefore, we used the general form of the dissipation-fluctuation theorem (Callen and Welton, [9]) for deriving the receiver noise temperature from the measured Y-factor.

4. Noise Temperature Measurements

All noise temperatures reported in this paper were measured with the same NbN HEB mixer. Compared to previously published results with this device [10] we were able to improve its performance mainly by improving the accuracy of the mounting of the HEB with respect to the center of the Si lens and by using a lower loss beamsplitter. It is worth mentioning that the device has shown no degradation in either the dc characteristics or the noise performance, although it has been already eight months under test.

In Fig. 3 the unpumped and pumped I-V curves of the HEB mixer at a temperature of 4.2 K are shown. The series resistance in the superconducting state is about 3 Ω. There is a first plateau in the IV-characteristic at a current of 45 μA that is followed by a second linear increase corresponding to a resistance of 40 Ω. Another plateau develops at a current of 55 μA. After the third almost linear increase, which corresponds to a resistance of 80 Ω, the maximum critical current of 90 μA is reached. The normal resistance of the HEB at the operation temperature was almost the same as at room temperature. This behavior is likely to be due to the existence of three patches in the superconducting film each with a different critical current. We speculate that two of them are situated under the contact pads. The critical current in those parts is reduced due to the proximity effect between NbN and gold. A tail seen in the resistive transition of the device below the critical temperature likely supports this tentative explanation.

We have measured the receiver noise temperature for different bias conditions and different LO powers. Low noise temperatures were usually found at a moderate bias voltage (around 1.8 mV and 22 μA) corresponding to an almost linear part of the IV-characteristic (region 1 in fig. 3). However, at smaller bias voltages (around 0.05 mV and 24 μA) corresponding to the nonlinear regime the noise temperature was usually somewhat lower (region 2 in fig. 3). At 2.5 THz we measured a lowest noise temperature of 2900 K in region 1 while in region 2 the lowest noise temperature was 2200 K. At 1.4 THz it was 2200 K (region 1) and 1600 K (region 2). The values for region 2 are corrected for the direct detection contribution which is significant while insignificant in region 1. The region 2 is very close to the unstable region of the IF signal (fig. 3). In the following part of this section we will discuss only the results for the region 1 which is better suited for radiometric applications (see section 5).

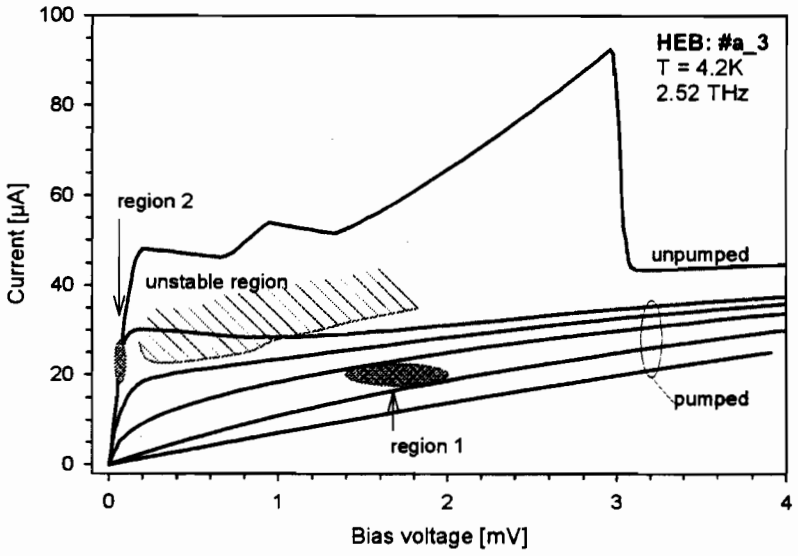

Fig. 3: Unpumped and pumped (at 2.5 THz) IV characteristics of the investigated HEB mixer. Also shown are the different regions with low noise temperatures and the unstable region (explanation see text).

In table 2 and fig. 4 the DSB receiver noise temperature is shown as a function of the LO frequency between 0.7 THz and 5.2 THz. Also shown in Fig. 4 is the DSB receiver noise temperature when corrected for the losses in the optical elements as given in table 3. In this case the increase is linear and follows closely the 10 hν/k line. This result suggests that the hybrid antenna of the mixer is frequency independent from 0.7 THz up to 5.2 THz.

Freq. [THz]	0.6929	1.3971	1.6266	2.5228	3.1059	4.2517	5.2456
T_{rec} DSB [K]	1500	2200	2600	2900	4000	5600	8800

Tab. 2: Measured DSB receiver noise temperatures at different frequencies.

We use the criterion $\lambda/2 \leq D$ (D =.130 μm) [5] for the cut-off at the low frequency side. For our antenna this yields the free space wavelength outside the silicon of 884 μm (0.34 THz). The shortest wavelength for which the spiral antenna is still working properly is about 10 times the inner radius at which the spiral deviates from the ideal shape [11]. In our case this is 1.3 μm yielding a lower wavelength limit of 44 μm (6.8 THz).

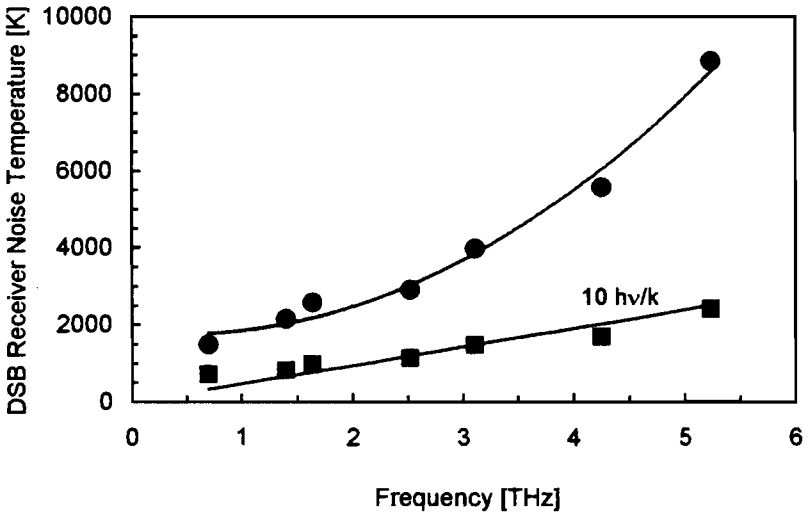

Fig.: 4: DSB receiver noise temperature as a function of frequency. The circles indicate the measured noise temperature while the squares correspond to the noise temperature corrected for losses in the optics.

According to table 2 the quartz filter and the Si lens give the major contributions to the total losses. Using a Zitex filter instead of the quartz filter could reduce the noise temperature by about 0.6– 1.4 dB in the frequency range from 0.7 THz to 2.5 THz. This for example would yield a DSB noise temperature of about 2400 K at 2.5 THz (loss of Zitex filter ≤0.5 dB [12]). This is comparable with other phonon cooled HEB mixers [13,14] as well as with Nb diffusion cooled HEB mixers [15]. However Zitex has a roll-off slightly above 2.5 THz [12]. Above this frequency a quartz filter has an

advantage. For the reduction of the loss in the Si lens no straightforward solution is available. One possibility to reduce the reflection could be the use of grooves and separation of a certain shape on the surface of the Si lens. This approach is discussed in Ref. 16.

	Loss [dB]						
Frequency	0.7 THz	1.4 THz	1.6 THz	2.5 THz	3.1 THz	4.3 THz	5.2 THz
Beamsplitter	0.1	0.2	0.3	0.6	0.7	1.2	1.2
TPX window	0.4	0.4	0.5	0.6	0.6	0.8	0.9
Quartz filter	1.1	1.8	1.9	1.2	1.3	1.5	1.9
Si lens (refl.)	1.5	1.5	1.5	1.5	1.5	1.5	1.5
Si lens (absorp.)	0.1	0.1	0.1	0.1	0.1	0.1	0.1
Sum	3.2	4.0	4.3	4.0	4.2	5.1	5.6

Table 2: Losses in the optics (data for the beamsplitter are calculated, data for the TPX window and the quartz filter are from the transmission curves as given by the manufacturer, data for the Si lens are estimated).

The LO power absorbed in the HEB was evaluated from the pumped and unpumped IV characteristics. We used the isothermal method described elsewhere [12]. An absorbed LO power around 100 nW was determined at all frequencies.

5. Sensitivity Fluctuation

It is instructive to determine not only the noise temperature but also the sensitivity fluctuation ΔT of a receiver. Fig. 5 shows the sensitivity fluctuation for the optimum bias (region 1 in fig. 2) at 1.4 THz. The first half of the scan is with the cold load in the signal path while the second half is with the hot load in the signal path. This scan documents the good stability of the laser LO. The temperature ΔT_{min} that corresponds to fluctuations of the total output power of the receiver is given by $\Delta T_{min} = T_{sys} / (\Delta\nu\ \tau_{int})^{1/2}$ [17] (bandwidth $\Delta\nu$ = 75 MHz, integration time τ_{int} = 2 ms). From the scan in fig. 5 we estimate a rms sensitivity fluctuation of 7.4 K, that is in a good agreement with the calculated value of 6.2 K. In comparison, the rms fluctuation sensitivity is about 30 K in region 2, for which the best noise temperature was measured (1600 K). The situation at 2.5 THz is similar. While in region 1 the sensitivity fluctuation is close to the theoretical limit it is up to 100 K in region 2. We attribute this dramatic increase of sensitivity fluctuations to an enhanced magnitude of rms noise at the device output. The region 2 corresponds to the strongly nonlinear operation regime when the impedance of HEB is very sensitive against small variations of the bias

voltage, LO power, and operation temperature. This was also experimentally found and is indicated in fig 2 by the much smaller area of region 2 compared to region 1. Instabilities of any of the operation parameters effect the operating point of the HEB and, consequently, the matching of the HEB to the IF network. This results in additional noise. Besides that there could be intrinsic reasons caused by physics of the detection and mixing process, e.g. switching of the bias current between different paths in a non-uniform film driven in the resistive state. However, at this stage a definite answer to the question about the origin of excess rms noise is not possible. Results of our measurements make clear that, although region 2 yields the better noise temperature, it is not readily suitable for radiometric applications.

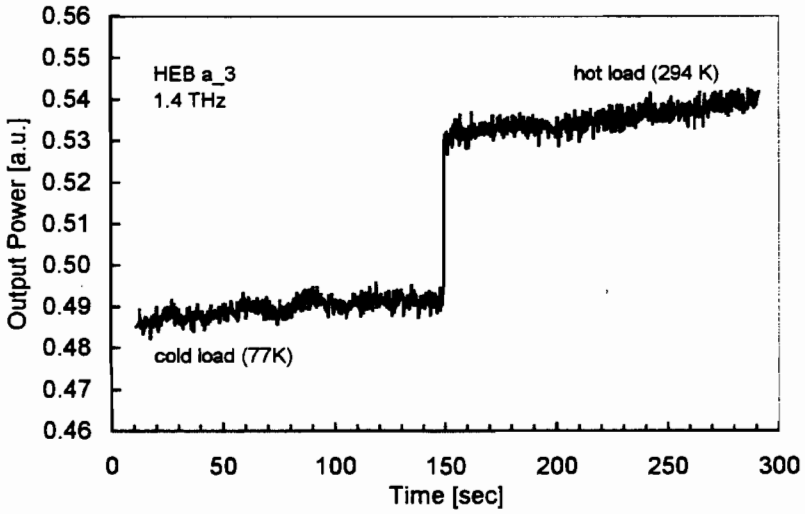

Fig. 5: Output noise of the HEB mixer as a function of time.

6. Conclusions

We have measured the noise temperature and fluctuation sensitivity of a phonon-cooled hot-electron bolometric mixer operated in different bias regimes in the frequency range from 0.7 THz to 5.2 THz. We demonstrated that the superlinear increase of the DSB noise temperature with frequency resulted from frequency dependent losses in coupling optics. When corrected for losses, the noise temperature of the mixer increased linearly with frequency with the slope 10 hν/k, thus suggesting that the hybrid antenna was frequency independent in the specified frequency range. We found two distinctive bias regimes resulting in fairly low noise temperature, of which only one provided fluctuation sensitivity corresponding to theoretical estimates. Our results show that it is possible to build a broadband HEB mixer with lowest noise temperatures.

Acknowledgment

We would like to thank U. Bartels for assistance with the mounting of the HEB and for assistance during the measurements.

References

[1] H. P. Röser, H.-W. Hübers, T. W. Crowe, W. C. B. Peatman, Infrared Phys. Technol. **35**, 451 (1994).
[2] A. L. Betz, R. T. Boreiko, Proc. of the 7th Int. Symp. on Space Terahertz Technology, 503 (1996).
[3] S. Cherednichenko, P Yagoubov, K. Il'in, G. Gol'tsman, E. Gershenzon, Proc. of the 8th Int. Symp. on Space Terahertz Technology, 245 (1997).
[4] S. Svechnikov, A. Verevkin, B. Voronov, E. Menschikov, E. Gershenzon, G. Gol'tsman, Proc. of the 9th Int. Symp. on Space Terahertz Technology, 45 (1998).
[5] J. D. Kraus, *Antennas*, McGraw-Hill, Inc., (1988).
[6] T. H. Büttgenbach, IEEE Trans. Microwave Theory Tech. **41**, 1750 (1993).
[7] H.-W. Hübers, G. W. Schwaab, H. P. Röser, Proc. 30th ESLAB Symp. „Submillimetre and Far-Infrared Space Instrumentation", ESA SP-388, 159 (1996).
[8] H.-W. Hübers, L. Töben, H. P. Röser, Rev. Sci. Instr. **69**, 290 (1998).
[9] A. R. Kerr, M. J. Feldman, S. K. Pan, Proc. of the 8th Int. Symp. on Space Terahertz Technology, 101 (1997).
[10] G. W. Schwaab, G. Sirmain, J. Schubert, H.-W. Hübers, G. Gol'tsman, S. Cherednichenko, A. Verevkin, E. Gershenzon, to appear in IEEE Trans. on Appl. Superconductivity (1999)
[11] T. H. Büttgenbach, R. E. Miller, M. J. Wengler, D. M. Watson, T. G. Phillips, IEEE Trans. On Microwave Theory Tech. **36**, 1720 (1988).
[12] B. Karasik, M. Gaidis, W. R. McGrath, B. Bumble, H. G. LeDuc, Proc. of the 8th Int. Symp. on Space Terahertz Technology, 55 (1997).
[13] P. Yagoubov, M. Kroug, H. Merkel, E. Kollberg, H.-W. Hübers, J. Schubert, G. Gol'tsman, E. Gershenzon, G. Schwaab, this volume (1999).
[14] P. Yagoubov, M. Kroug, H. Merkel, E. Kollberg, J. Schubert, H.-W. Hübers, G. Schwaab, G. Gol'tsman, E. Gershenzon, to appear in IEEE Trans. on Appl. Superconductivity (1999).
[15] B. Karasik, M. Gaidis, W. R. McGrath, B. Bumble, H. G. LeDuc, Appl. Phys. Lett. **71**, 1567 (1997).
[16] G. Schwaab, H.-W. Hübers, J. Schubert, G. Gol'tsman, A. Semenov, A. Verevkin, S. Cherednichenko, E. Gershenzon, this volume (1999)
[17] J. D. Kraus, *Radio Astronomy*, 2nd ed., Powell (1986).